Evolution trajectories of snake genes and genomes revealed by comparative analyses of five-pacer viper

Wei Yin[1,*], Zong-ji Wang[2, 3, 4, 5,*], Qi-ye Li[3, 4, 6], Jin-ming Lian[3], Yang Zhou[3], Bing-zheng Lu[7], Li-jun Jin[3], Peng-xin Qiu[7], Pei Zhang[3], Wen-bo Zhu[7], Bo Wen[8], Yi-jun Huang[7], Zhi-long Lin[8], Bi-tao Qiu[3, 9], Xing-wen Su[7], Huan-ming Yang[8,9], Guo-jie Zhang[3, 4, 10], Guang-mei Yan[7,#], Qi Zhou[2,11, #]

1. Department of Biochemistry, Zhongshan School of Medicine, Sun Yat-sen University, Guangzhou, 510089, China.
2. Life Sciences Institute, The Key Laboratory of Conservation Biology for Endangered Wildlife of the Ministry of Education, Zhejiang University, Hangzhou, 310058, China.
3. China National Genebank, BGI-Shenzhen, Shenzhen, 518083, China.
4. State Key Laboratory of Genetic Resources and Evolution, Kunming Institute of Zoology, Chinese Academy of Sciences, Kunming, China.
5. School of Bioscience & Bioengineering, South China University of Technology, Guangzhou, 510006, China.
6. Centre for GeoGenetics, Natural History Museum of Denmark, University of Copenhagen, Øster Voldgade 5–7, 1350 Copenhagen K, Denmark.
7. Department of Pharmacology, Zhongshan School of Medicine, Sun Yat-sen University, Guangzhou, 510089, China.
8. BGI-Shenzhen, Shenzhen, 518083, China.
9. James D. Watson Institute of Genome Sciences, Hangzhou 310058, China
10. Centre for Social Evolution, Department of Biology, University of Copenhagen, Universitetsparken 15, DK-2100 Copenhagen, Denmark.
11. Department of Integrative Biology, University of California, Berkeley, Berkeley, CA94720, United States

[*] These authors contributed equally to the work

[#] To whom correspondence should be addressed: zhouqi1982@zju.edu.cn or ygm@mail.sysu.edu.cn

Abstract

Snake's numerous fascinating features distinctive from other tetrapods necessitate a rich history of genome evolution that is still obscure. To address this, we report the first high-quality genome of a viper, *Deinagkistrodon acutus* and comparative analyses using other species from major snake and lizard lineages. We map the evolution trajectories of transposable elements (TEs), developmental genes and sex chromosomes onto the snake phylogeny. TEs exhibit dynamic lineage-specific expansion. And in the viper many TEs may have been rewired into the regulatory network of brain genes, as shown by their associated expression with nearby genes in the brain but not in other tissues. We detect signatures of adaptive evolution in olfactory, venom and thermal-sensing genes, and also functional degeneration of genes associated with vision and hearing. Many *Hox* and *Tbx* limb-patterning genes show evidence of relaxed selective constraints, and such genes' phylogenetic distribution supports fossil evidence for a successive loss of forelimbs then hindlimbs during the snake evolution. Finally, we infer that the Z and W sex chromosomes had undergone at least three recombination suppression events at the ancestor of advanced snakes, with the W chromosomes showing a gradient of degeneration from basal to advanced snakes. These results, together with all the genes identified as undergoing adaptive or degenerative evolution episodes at respective snake lineages forge a framework for our deep understanding into snakes' molecular evolution history.

Snakes have undergone massive adaptive radiation with ~3400 extant species successfully inhabiting almost all continents except for the polar regions[1]. This process has culminated in 'advanced snakes' (Caenophidia, ~3000 species), involved numerous evolutionary changes in body form, chemo-/thermo- perception, venom and sexual reproductive systems, which together distinguish snakes from majorities of other Squamates (lizards and worm lizards). Some of these dramatic changes can be tracked from fossils, which established that the ancestor of snakes had already evolved a elongated body plan, probably as an adaptation to a burrowing and crawling lifestyle, but had lost only the forelimbs[2-4]. Extant boa and python species retain rudimentary hindlimbs, while advanced snakes have completely lost them. The limblessness, accompanied by degeneration in visual and auditory perception have not compromised snakes' dominant role as top predators, largely due to the evolution of infrared sensing and/or venom, and the development of corresponding facial pit and fangs (specialized teeth for venom injection) independently in different lineages[5,6].

These extreme adaptations have sparked strong and standing interest into their genetic basis. Snakes are used as a model for studying various basic questions like mechanisms of axial patterning and limb development[3,7,8], 'birth-and-death' of venom proteins[9-11], and also sex chromosome evolution[12]. Cytogenetic findings in snakes first drove Ohno to propose that sex chromosomes in vertebrates evolved from ancestral autosomes[13], like those of insects[14] and plants[15]. Our insights into these questions have been recently advanced by the application of next-generation sequencing. Analyses of python and king cobra genomes and transcriptomes have uncovered the metabolic gene repertoire involved in feeding, and inferred massive expansion and adaptive evolution of toxin families in elapids (an 'advanced' group)[10,16]. However, comparative studies of multiple snake genomes unraveling their evolutionary trajectories since the divergence from lizards are lacking, and so far only a few specific developmental 'toolbox' (e.g., *Hox*[7,17,18] and Fgf signaling pathway[19]) genes have been studied between snakes and lizards. This hampers our comprehensive understanding into the molecular basis of stepwise or independent acquisition of snake specific traits. We bridge this gap here by deep-sequencing the genomes and transcriptomes of five-pacer viper (*Deinagkistrodon*

81 *acutus*, **Figure 1A**), a member of the Viperidae family. This pit viper is a paragon of
82 infrared sensing, heteromorphic ZW sex chromosomes, and distinctive types of fangs and
83 toxins (its common name exaggerates that victims can walk no more than five paces)
84 from other venomous snake families[6,20]. Despite the intraspecific differences within the
85 same family, comparative analyses to the available genomes of three other major snake
86 family species, i.e., *Boa constrictor* (Boidae family)[21], *Python bivittatus* (Pythonidae
87 family)[16], *Ophiophagus hannah* (Elapidae family)[10] and several reptile outgroups should
88 recapitulate the major genomic adaptive or degenerative changes occurred in the ancestor
89 and along individual branches of snake families, and would also promote current
90 antivenom therapy and drug discovery (e.g., thrombolytics) out of the viper toxins[22].
91
92 **Evolution of snake genome architecture**
93 We sequenced a male and a female five-pacer viper to extremely high-coverage (♀ 238
94 fold, ♂114 fold, **Supplementary Table 1**), and estimated the genome size to be 1.43Gb
95 based on k-mer frequency distribution[23] (**Supplementary Table 2, Supplementary**
96 **Figure 1**). Fewer than 10% of the reads, which have a low quality or are probably
97 derived from repetitive regions, were excluded from the genome assembly
98 (**Supplementary Table 3**). We generated a draft genome using only male reads for
99 constructing the contigs, and female long-insert (2kb~40kb) library reads for joining the
100 contigs into scaffolds. It has an assembled size of 1.47Gb, with a slightly better quality
101 than the genome using purely female reads. It has high continuity (contig N50: 22.42kb,
102 scaffold N50: 2.12Mb) and integrity (gap content 5.6%, **Supplementary Table 4**), thus
103 was chosen as the reference genome for further analyses. It includes a total of 21,194
104 predicted protein-coding genes, as estimated using known vertebrate protein sequences
105 and massive transcriptome data generated in this study from eight tissues (**Figure 1A,**
106 **Materials and Methods**). For comparative analyses, we also annotated 17,392
107 protein-coding genes in the boa genome (the SGA version from[21]). 80.84% (17,134) of
108 the viper genes show robust expression (normalized expression level RPKM>1) in at
109 least one tissue, comparable to the value of 70.77% in king cobra (**Supplementary Table**
110 **5**). Based on 5,353 one-to-one orthologous gene groups of four snake species (five-pacer

111 viper, boa[21], python[16], king cobra[10]), green anole lizard[24] and several other sequenced
112 vertebrate genomes (**Materials and Methods**), we constructed a phylogenomic tree with
113 high bootstrapping values at all nodes (**Figure 1B**). We estimated that advanced snakes
114 diverged from boa and python about 66.9 (47.2~84.4) million years ago (MYA), and
115 five-pacer viper and king cobra diverged 44.9 (27.5~65.0) MYA assuming a molecular
116 clock. These results are consistent with the oldest snake and viper fossils from 140.8 and
117 84.7 MYA, respectively[25].
118 The local GC content of snakes (boa and five-pacer viper) shows variation (GC
119 isochores) similar to the genomes of turtles and crocodiles, and intermediate between
120 mammals/birds and lizard (**Figure 1C, Supplementary Figure 2**), confirming the loss of
121 such a genomic feature in lizard among tetrapods[24]. Cytogenetic studies showed like most
122 other snakes, the five-pacer viper karyotype has 2n=36 (16 macro- and 20
123 micro-chromosomes) chromosomes[26], with extensive inter-chromosomal conservation
124 with the lizard[27]. This enables us to organize 56.50% of the viper scaffold sequences into
125 linkage groups, based on their homology with sequences of known green anole lizard
126 macro-chromosomes (**Supplementary Table 6**). As expected, autosomal sequences have
127 the same read coverage in both sexes, whereas scaffolds inferred to be located on the
128 viper Z chromosome (homologous to green anole lizard chr6) have coverage in the
129 female that is half that in the male (**Figure 1C**). Additionally, the frequency of
130 heterozygous variants on the Z chromosome is much lower in the female than in the male
131 (0.005% vs 0.08%, *P*-value<2.2e-16, Wilcoxon signed rank test) due to the nearly
132 hemizygous state of Z chromosome in female, while those of autosomes (~0.1%) are very
133 similar between sexes. These results indicated that our assembly mostly assigns genes to
134 the correct chromosome, and this is further supported by comparisons of 172 genes'
135 locations with previous fluorescence *in situ* hybridization results (**Supplementary Data**
136 **1**)[27]. They also suggest that the viper sex chromosomes are highly differentiated from
137 each other (see below).
138 47.47% of the viper genome consists of transposable element sequences (TEs),
139 higher than any other snakes so far analyzed (33.95~39.59%), which cannot be explained
140 solely by the higher assembly quality than that of the other species genome

141 sequences[10,16,21] **(Supplementary Table 7-8)**. These are mostly long interspersed
142 elements (LINE, 13.84% of the genome) and DNA transposons (7.96%, **Supplementary**
143 **Table 7**). Sequence divergence of individual families from inferred consensus sequences
144 uncovered recent rampant activities in the viper lineage of LINEs (CR1), DNA
145 transposons (hAT and TcMar) and retrotransposons (Gypsy and DIRS). In particular,
146 there is an excess of low-divergence (<10% divergence level) CR1 and hAT elements in
147 the viper genome only (**Figure 2A**). We also inferred earlier propagation of TEs shared
148 by viper and king cobra, which thus probably occurred in the ancestor of advanced
149 snakes. Together, these derived insertions resulted in an at least three-fold difference in
150 the CR1 and hAT content between viper and more basal-branching snakes like boa and
151 python (**Figure 2B**). While boa and python have undergone independent expansion of L2
152 and CR1 repeats, so that their overall LINE content is at a similar level to that of the
153 viper and cobra (**Figure 2A, Supplementary Table 7**).
154 These TEs are presumably silenced through epigenetic mechanisms to prevent their
155 deleterious effects of transposition or mediating genomic rearrangements. Indeed, very
156 few are transcribed in all of the tissue examined, except, unexpectedly in brain (**Figure**
157 **2C**). This brain-specific expression prompted us to test whether some snake TE families
158 might have been co-opted into brain gene regulatory networks. Focusing on highly
159 expressed (RPKM>5) TEs' that are located within 5kb flanking regions of genes, we
160 found that these nearby genes also show a significantly higher expression in brain than
161 any other tissues (*P-value*<1.1e-40, Wilcoxon test, **Supplementary Figure 3**). The
162 expression levels of individual genes are strongly correlated (*P-value*<1.35e-08,
163 Spearman's test) with those of nearby TE's. These genes are predominantly enriched
164 (*Q-value* < 0.05, Fisher's Chi-square test, **Supplementary Data 2**) in functional domains
165 of 'biological process' compared to 'cellular component' and 'molecular function', and
166 particularly enriched categories include environmental response ('response to organic
167 substance', 'regulation of response to stimulus' and 'sensory perception of light stimulus')
168 and brain signaling pathways ('neuropeptide signaling pathway', 'opioid receptor
169 signaling pathway' and 'regulation of cell communication' etc.). Further experimental
170 studies are required to elucidate how some of these TEs evolved to regulate the brain

171 gene expression; these results nevertheless highlighted the evolution dynamics and
172 potential functional contribution of TEs in shaping the snake genome evolution.
173
174 **Evolution of snake genes and gene families**
175 To pinpoint the critical genetic changes underlying the phenotypic innovations of snakes,
176 we next mapped protein coding genes' gain and loss (**Figure 1B**), signatures of adaptive
177 or degenerative evolution (**Figure 3A**) measured by their ratios (ω) of nonsynonymous vs.
178 synonymous substitution rates (**Supplementary Data 3**) onto the phylogenetic tree. We
179 inferred a total of 1,725 gene family expansion and 3,320 contraction events, and
180 identified 610 genes that appear to have undergone positive selection (PSG) and 6149
181 with relaxed selective constraints (RSG) at different branches, using a likelihood model
182 and conserved lineage-specific test[28]. Genes of either scenario were separated for
183 analyzing their enriched gene ontology (GO) and mouse orthologs' mutant phenotype
184 (MP) terms, assuming most of them have a similar function in snakes.
185 Significantly (*P-value*<0.05, Fisher's exact test) enriched MP terms integrated with
186 their branch information illuminated the molecular evolution history of snake-specific
187 traits (**Figure 3A**). For example, as adaptations to a fossorial lifestyle, the four-legged
188 snake ancestor[29] had evolved an extreme elongated body plan without limbs, and also
189 fused eyelids ('spectacles', presumably for protecting eyes against soil[30]). The latter is
190 supported by the results for the PSG genes *Ereg*, and RSGs *Cecr2* and *Ext1* at the snake
191 ancestor branch (**Supplementary Data 4**), whose mouse mutant phenotype is shown as
192 prematurely opened or absent eyelids. The limbless body plan has already driven many
193 comparisons of expression domains and coding-sequences of the responsible *Hox* genes
194 between snakes and other vertebrates[7,17]. We here refined the analyses to within-snake
195 lineages, focusing on sequence evolution of *Hox* and other genes involved in limb
196 development and somitogenesis. We annotated the nearly complete sequences of 39 *Hox*
197 genes organized in four clusters (*HoxA*-*HoxD*) of the five-pacer viper. Compared to the
198 green anole lizard, the four studied snake species have *Hox* genes whose sizes are
199 generally reduced, due to the specific accumulation of DNA transposons in the lizard's
200 introns and intergenic regions (**Supplementary Figure 4**). However, snakes have

201 accumulated particularly higher proportions of simple tandem repeat and short
202 interspersed element (SINE) sequences within *Hox* clusters (**Supplementary Figure 5**),
203 either as a result of relaxed selective constraints and/or evolution of novel regulatory
204 elements. We identified 11 *Hox* genes as RSGs and one (*Hoxa9*) as PSG (**Figure 3B**).
205 Their combined information of gene function and affected snake lineage informed the
206 stepwise evolution of snake body plan. In particular, *Hoxa5*[31], *Hoxa11*[32] and *Tbx5*[33]
207 which specifically pattern the forelimbs in mouse, have been identified as RSGs in the
208 common ancestor of all four snakes. While *Hoxc11* and *Tbx4*[34], which pattern the
209 hindlimbs in mouse, and many other limb-patterning genes (e.g. *Gli3*, *Tbx18*, *Alx4*) were
210 identified as RSGs that evolved independently on snake external branches (**Figure 3B,**
211 **Supplementary Data 4**). These results provide robust molecular evidence supporting the
212 independent loss of hindlimbs after the complete loss of forelimbs in snake ancestors. In
213 the snake ancestor branch, we also identified RSGs *Hoxa11, Hoxc10* and *Lfng*, which are
214 respectively associated with sacral formation[35], rib formation[8] and somitogenesis speed[36]
215 in vertebrates. Their changed amino acids and the expression domains that have expanded
216 in snakes relative to lizards[17,19] might have together contributed to the
217 'de-regionalization'[17] and elongation of the snake body plan. In several external branches,
218 we identified *Hoxd13* independently as RSG. Besides its critical roles in limb/digit
219 patterning[37], it is also associated with termination of somitogenesis signal and is
220 specifically silenced at the snake tail relative to lizard[7]. This suggests that body
221 elongation may have evolved more than once among snake lineages. Overall,
222 limb/digit/tail development MP terms are significantly enriched in RSGs at both ancestral
223 and external branches of snakes (**Figure 3A**), and we identified many such genes at
224 different snake lineages for future targeted experimental studies (**Supplementary Table 9,**
225 **Supplementary Data 4**).
226 Another important adaption to snakes' ancestrally fossorial and later ground surface
227 lifestyle is the shift of their dominant source of environmental sensing from
228 visual/auditory to thermal/chemical cues. Unlike most other amniotes, extant snake
229 species do not have external ears, and some basal species (e.g., blindsnake) have
230 completely lost their eyes. Consistently, we found MP terms associated with hearing/ear

231 and vision/eye phenotypes (e.g., abnormal ear morphology, abnormal vision, abnormal
232 cone electrophysiology) are enriched among RSGs along all major branches of snakes
233 starting from their common ancestor (**Figure 3A, Supplementary Figure 6,**
234 **Supplementary Data 4**). Gene families that have contracted in the ancestor of four
235 studied snake species, and specifically in the viper, are also significantly (*Q-value*<
236 9.08e-4, Fisher's Exact Test) enriched in gene ontologies (GO) of 'sensory perception of
237 light stimulus (GO:0050953)' or 'phototransduction (GO:0007602)' (**Figure 1C,**
238 **Supplementary Data 5**). In particular, only three (*RH1, LWS* and *SWS1*) out of 13 opsin
239 genes' complete sequences can be identified in the viper genome, consistent with the
240 results found in python and cobra[16]. By contrast, infrared receptor gene *TRPA1*[5] and
241 ubiquitous taste-signaling gene *TRPM5*[38] have respectively undergone adaptive evolution
242 in five-pacer viper and the ancestor of boa and python. Gene families annotated with the
243 GO term 'olfactory receptor (OR) activity' have a significant (*Q-value* < 1.63e-4, Fisher's
244 Exact Test) expansion in all snake species studied and at some of their ancestral nodes,
245 except for the king cobra (**Supplementary Data 6**). In the boa and viper, whose genome
246 sequences have much better quality than the other two snake genomes, we respectively
247 annotated 369 and 412 putatively functional OR genes, based on homology search and
248 the characteristic 7-TM (transmembrane) structure (**Materials and Methods**). Both
249 terrestrial species have an OR repertoire predominantly comprised of class II OR families
250 (OR1-14, presumably for binding airborne molecules, **Figure 3C**), and their numbers are
251 much higher than the reported numbers in other Squamate genomes[39]. Some (ranging
252 from 18 to 24) class I (OR51-56, for water-borne molecules) genes have also been found
253 in the two species, indicating this OR class is not unique to python as previously
254 suggested[39]. Compared with the green anole lizard, the boa and viper exhibit a significant
255 (P<0.05, Fisher's exact test) size expansion of OR family 5, 11 and 14, and also a bias
256 towards being located on the Z chromosome (**Figure 3C**), leading to higher expression of
257 many OR genes in males than in females (see below). In particular, OR5 in the viper
258 probably has experienced additional expansion events and become the most abundant
259 (with 71 members) family in the genome. Intriguingly, this family is specifically enriched
260 in birds of prey[40] relative to other birds, and in non-frugivorous bats vs. frugivorous

261 bats[41]. Therefore, its expansion in the five-pacer viper could have been positively selected
262 for a more efficient detection of prey.
263 Besides acute environmental sensing, specialized fangs[6] and venoms[11] (e.g,
264 hemotoxins of viper or neurotoxins of elapid) arm the venomous snakes (~650 species) to
265 immediately immobilize the much larger prey for prolonged ingestion, which probably
266 comprised one of the most critical factors that had led to the advanced snakes' species
267 radiation. It has been proposed that the tremendous venom diversity probably reflects
268 snakes' local adaption for the prey[42] and was generated by changes in the expression of
269 pre-existing or duplicated genes[11,43]. Indeed, we found that the five-pacer viper's venom
270 gland gene repertoire has a very different composition comparing to other viper[44] or
271 elapid species[10] (**Figure 3D**). We have annotated a total of 35 venom genes or gene
272 families using all the known snake venom proteins as the query. Certain gene families,
273 including snake venom metalloproteinases (SVMP), C-type lectin-like proteins (CLPs),
274 thrombin-like snake venom serine proteinases (TL), Kunitz and disintegrins, have more
275 genomic copies in the five-pacer viper than other studied snakes or the green anole lizard
276 (**Supplementary Table 10**); while characteristic elapid venom genes like three-finger
277 toxins (3FTx) are absent from the viper genome. Most venom proteins of both the viper
278 and king cobra have expression restricted to venom or accessary glands, and for both
279 species this is particularly seen for those genes that originated in the ancestor of snakes or
280 of advanced snakes (**Figure 3D**). But for elapid or viper specific venom genes, i.e., those
281 that originated more recently, they usually express in the liver of the other species. Such
282 cases include FactorV, FactorX of king cobra and PLA2-2A of viper (**Figure 3D**). This
283 suggests that these venom genes may have originated from metabolic proteins and
284 undergone neo-/sub-functionalization, with altered expression.
285
286 **Evolution of snake sex chromosomes**
287 Different snake species exhibit a continuum of sex chromosome differentiation: pythons
288 and boas possess homomorphic sex chromosomes, which is assumed to be the ancestral
289 state; the lack of differentiation between the W and Z chromosomes suggests that most
290 regions of this chromosome pair recombine like the autosomes[45]. Advanced snakes

291 usually have heteromorphic sex chromosomes that have undergone additional
292 recombination suppressions[45,46]. We found the five-pacer viper probably has suppressed
293 recombination throughout almost the entire sex chromosome pair, as the read coverage in
294 the female that we sequenced is half that in the male (**Figure 1C, Figure 4**). By contrast,
295 boa's homologous chromosomal regions show a read coverage pattern that does not differ
296 from that of autosomes. Assuming that these two species share the same ancestral snake
297 sex-determining region, this suggests that that region is not included in our current
298 chromosomal assembly.

299 In plants, birds and mammals, it has been found that recombination suppression
300 probably occurred by a succession of events. This has led to the punctuated accumulation
301 of excessive neutral or deleterious mutations on the Y or W chromosome by genetic drift,
302 and produced a gradient of sequence divergence levels over time, which are termed
303 'evolutionary strata'[47-49]. Advanced snakes have been suggested to have at least two
304 strata[12]. One goal of our much better genome assembly of the five-pacer viper compared
305 to those of any other studied advanced snakes[10,12] (**Supplementary Table 4**) was to
306 reconstruct a fine history of snake sex chromosome evolution. We assembled 77Mb
307 Z-linked and 33Mb W-linked scaffolds (**Materials and Methods**). The reduction of
308 female read coverage along the Z chromosome suggests there is a substantial divergence
309 between Z- and W- linked sequences, and this would enable the assembly of two
310 chromosomes' scaffolds in separate. Mapping the male reads confirmed that the inferred
311 W-linked scaffold sequences are only present in female (**Supplementary Figure 7**).
312 Their density and pairwise sequence divergence values within putative neutral regions
313 along the Z chromosome indicate at least two 'evolution strata', with the older stratum
314 extending 0~56Mb, and the younger one extending 56~70Mb. The boundary at 56Mb
315 region can be also confirmed by analyses of repetitive elements on the Z chromosome
316 (see below). Consistently, identifiable W-linked fragments are found at the highest
317 density per megabase in the latter (**Figure 4**), suggesting that this region has suppressed
318 recombination more recently. The older stratum includes much fewer identifiable
319 fragments that can resolve the actual times of recombination suppression events. To study
320 this region further, we inspected the homologous Z-linked region, whose recombination

321 has also been reduced, albeit to a much smaller degree than the W chromosome, after the
322 complete suppression of recombination between Z/W in females. In addition, Z
323 chromosome is biasedly transmitted in males. As males usually have a higher mutation
324 rate than females, due to many more rounds of DNA replication during spermatogenesis
325 than oogenesis ('male-driven evolution')[50], Z-linked regions are expected to have a
326 generally higher mutation rate than any other regions in the genome. This male-driven
327 evolution effect has been demonstrated in other snake species[12], and also been validated
328 for the snakes inspected in this study (**Supplementary Figure 8**). As a result, we
329 expected regions in older strata should be more diverged from their boa autosome-like
330 homologs than those in the younger strata. This enabled us to identify another stratum
331 (0~42Mb, stratum 2, S2 in **Figure 4**) and demarcate the oldest one (42~56Mb, S1), by
332 estimating the sequence conservation level (measured by LASTZ alignment score, blue
333 line) between the Z chromosomes of boa and viper. The Z-linked region in the inferred
334 oldest stratum S1 exhibits the highest sequence divergence with the homologous
335 W-linked region, and also the highest proportion of repetitive elements (CR1, Gypsy and
336 L1 elements; **Figure 4** shows the example of Gypsy; other repeats are shown in
337 **Supplementary Figure 9**). This can be explained by the effect of genetic drift[51], which
338 has been acting on the Z-linked S1 for the longest time since it reduced recombination
339 rate in females. As a result, the accumulated repeats of S1 also tend to have a higher
340 divergence level from the inferred ancestral consensus sequences compared to nearby
341 strata (**Figure 4**). Unexpectedly, a similar enrichment was found in the homologous
342 region of S1 in boa, despite being a recombining region and exhibiting the same coverage
343 depth between sexes (**Figure 4**, **Supplementary Figure 9**). This indicates the pattern is
344 partially contributed by the ancestral repeats that had already accumulated on the
345 proto-sex chromosomes of snake species. Since our current viper sex chromosomal
346 sequences used the green anole lizard chromosome 6 as a reference, rearrangements
347 within this chromosome make it impossible to test whether S2 encompasses more than
348 one stratum.
349 We dated the three resolved strata by constructing phylogenetic trees with
350 homologous Z- and W- linked gene sequences of multiple snake species. Combining the

351 published CDS sequences of pygmy rattlesnake (Viperidae family species) and garter
352 snake (Colubridae family species)[12], we found 31 homologous Z-W gene pairs,
353 representing the three strata. All of them clustered by chromosome (i.e., the Z-linked
354 sequences from all the species cluster together, separately from the W-linked ones) rather
355 than by species (**Supplementary Figure 10-12**). This indicates that all three strata
356 formed before the divergence of advanced snakes, and after their divergence from boa
357 and python, i.e., about 66.9 million years ago (**Figure 1C**).
358 We found robust evidence of functional degeneration on the W chromosome. It is
359 more susceptible to the invasion of TEs: the assembled sequences' overall repeat content
360 is at least 1.5 fold higher than that of the Z chromosome, especially in the LINE L1 (2.9
361 fold) and LTR Gypsy families (4.3 fold) (**Supplementary Table 11 and Supplementary**
362 **Figure 13**). Of 1,135 Z-linked genes, we were only able to identify 137 W-linked
363 homologs. Among these, 62 (45.26%) have probably become pseudogenes due to
364 nonsense mutations (**Supplementary Table 12**). W-linked loci generally transcribe at a
365 significantly (*P-value*<0.0005, Wilcoxon test) lower level, with pseudogenes transcribing
366 even lower relative to the autosomal or Z-linked loci regardless of the tissue type
367 (**Supplementary Figure 14-15**). Given such a chromosome-wide gene loss, like other
368 snakes[12] or majority of species with ZW sex chromosomes[52], the five-pacer viper shows a
369 generally male-biased gene expression throughout the Z-chromosome and probably has
370 not evolved global dosage compensation (**Supplementary Figure 16**).
371
372 **Discussion**
373 The 'snake-like' body plan has evolved repeatedly in other tetrapods (e.g., worm lizard
374 and caecilians), in which limb reduction/loss seems to have always been accompanied by
375 the body elongation. For example, several limb-patterning *Hox* genes (*Hoxc10*, *Hoxd13*)
376 identified as RSG also have been characterized by previous work with a changed
377 expression domain along the snake body axis[7,17]. Another RSG *Hoxa5* which is involved
378 in the forelimb patterning[31], also participates in lung morphogenesis[53]. It might have been
379 involved in the elimination of one of the snake lungs during evolution. Therefore, the
380 newly identified PSGs and RSGs throughout the snake phylogeny in this work

381 (**Supplementary Data 3-4, Supplementary Table 9**) can provide informative clues for
382 future experimental work to use snake as an emerging 'evo-devo' model[54] to understand
383 the genomic architecture of developmental regulatory network of organogenesis, or the
384 crosstalk between these networks.

385 Like many of its other reptile relatives, the snake ancestor is very likely to determine
386 the sex by temperature and does not have sex chromosomes. Extant species Boa can still
387 undergo occasional parthenogenesis and is able to produce viable WW offspring[55],
388 consistent with its the most primitive vertebrate sex chromosome pair reported to date. In
389 the ancestor of advanced snakes, we inferred that there were at least three recombination
390 suppressions occurred between Z/W, leading to a generally degenerated W chromosome
391 that we have observed in five-pacer viper. How snakes genetically determine the sex
392 would be a rather intriguing question to study in future.

393

394 **Materials and Methods**

395 **Genome sequencing and assembly**

396 All animal procedures were carried out with the approval of China National Genebank
397 animal ethics committee. We extracted genomic DNAs from blood of a male and a
398 female five-pacer viper separately. A total of 13 libraries with insert sizes ranging from
399 250bp to 40kb were constructed using female DNA, and 3 libraries with insert sizes from
400 250 bp to 800 bp were constructed using male DNA. We performed paired-end
401 sequencing (HiSeq 2000 platform) following manufacturer's protocol, and produced 528
402 Gb raw data (357 Gb for female and 171 Gb for male). We estimated the genome size
403 based on the K-mer distribution. A K-mer refers to an artificial sequence division of K
404 nucleotides iteratively from sequencing reads. The genome size can then be estimated
405 through the equation G=K_num/Peak_depth, where the K_num is the total number of
406 K-mer, and Peak_depth is the expected value of K-mer depth[56]. We found a single main
407 peak in the male K-mer (K=17) frequency distribution and an additional minor peak in
408 the female data, the latter of which probably results from the divergence between W and
409 Z chromosomes **(Supplementary Figure 1)**. Based on the distribution, we estimated that
410 the genome size of this species is about 1.43 Gb **(Supplementary Table 2)**, comparable

411 to that of other snakes (1.44 Gb and 1.66Gb for Burmese python and King cobra[10,16],
412 respectively).
413 After filtering out low-quality and duplicated reads, we performed additional filtering
414 using the following criteria: we excluded the reads from short-insert libraries (250, 500,
415 800 bp) with 'N's over 10% of the length or having more than 40 bases with the quality
416 lower than 7, and the reads from large-insert libraries (2 kb to 40 kb) with 'N's over 20%
417 of the length or having more than 30 bases with the quality lower than 7. Finally, 109.20
418 Gb (73X coverage) male reads and 148.49Gb (99X coverage) female reads were retained
419 for genome assembly **(Supplementary Table 1)** using SOAPdenovo[57]
420 (http://soap.genomics.org.cn). To assemble the female and male genomes, reads from
421 small-insert libraries of the female and male individual were used for contig construction
422 separately. Then read-pairs from small- and large-insert libraries were utilized to join the
423 contigs into scaffolds. We also used female long-insert libraries to join the male contigs
424 into the longer scaffolds. At last, small-insert libraries of female and male individuals
425 were used for gap closure for their respective genomes. The final assemblies of female
426 and male have a scaffold N50 length of 2.0 Mb and 2.1 Mb respectively, and the gap
427 content of the two genomes are both less than 6% (♀ 5.29%, ♂ 5.61%)**(Supplementary**
428 **Table 4)**.
429 To access the assembly quality, reads from small-insert libraries that passed our
430 filtering criteria were aligned onto the two assemblies using BWA[58] (Version: 0.5.9-r16)
431 allowing 8 mismatches and 1 indel per read. A total of ~97% reads can be mapped back
432 to the draft genome (**Supplementary Table 3**), spanning 98% of the assembled regions
433 excluding gaps (**Supplementary Table 13**), and most genomic bases were covered by
434 about 80X reads **(Supplementary Figure 17)**. Thus we conclude that we have assembled
435 most part of the five-pacer viper genome. To further test for potential mis-joining of the
436 contigs into scaffolds, we analyzed the paired-end information and found that 57% of the
437 paired-end reads can be aligned uniquely with the expected orientation and distance. This
438 proportion of the long insert library is significantly lower than that from the short insert
439 libraries due to a circulization step during the library construction. When such
440 paired-ends were excluded, the proportion increased to 94.98% (**Supplementary Table**

441 **3**). Overall, these tests suggested that the contigs and scaffolds are consistent with the
442 extremely high density of paired-end reads, which in turn indicated the high-quality of
443 the assembly.

444 Previous cytogenetic studies showed that snake genomes show extensive
445 inter-chromosomal conservation with lizard[27,45]. Thus we used the chromosomal
446 information from green anole lizard[24] as a proxy to assign the snake scaffolds. We first
447 constructed their orthologous relationship combining information of synteny and
448 reciprocal best BLAST hits (RBH). Then gene coordinates and strandedness from the
449 consensus chromosome were used to place and orient the snake scaffolds. Furthermore,
450 we linked scaffolds into chromosomes with 600 'N's separating the adjacent scaffolds. In
451 total, 625 five-pacer viper scaffolds comprising 832Mb (56.50% scaffolds in length) were
452 anchored to 5 autosomes and Z chromosome (**Supplementary Table 6**).

453

454 **Repeat and gene annotation**

455 We identified the repetitive elements in the genome combining both homology-based and
456 *de novo* predictions. We utilized the 'Tetrapoda' repeat consensus library in Repbase[59] for
457 RepeatMasker (http://www.repeatmasker.org) to annotate all the known repetitive
458 elements in the five-pacer viper genome. In order to maximize the identification and
459 classification of repeat elements, we further used RepeatModeler
460 (http://www.repeatmasker.org/RepeatModeler.html) to construct the consensus repeat
461 sequence libraries of the green anole lizard, boa and five-pacer viper, then used them as a
462 query to identify repetitive elements using RepeatMasker. Finally, we retrieved a
463 non-redundant annotation for each species after combining all the annotation results
464 using libraries of 'Tetrapoda', 'green anole lizard', 'boa' and 'five-pacer viper'. For the
465 purpose of comparison, we ran the same pipeline and parameters in all the snake and
466 lizard genomes as shown in **Supplementary Table 7**. To provide a baseline estimate for
467 the sequence divergence of TEs from the snake ancestral status, we first merged the
468 genomes from boa and five-pacer viper, and constructed the putative ancestral consensus

469 sequences using RepeatModeler. Then TE sequences of each snake species were aligned
470 to the consensus sequence to estimate their divergence level using RepeatMasker.
471 For gene annotation, we combined resources of sequence homology, *de novo*
472 prediction and transcriptome to build consensus gene models of the reference genome.
473 Protein sequences of green lizard, chicken and human were aligned to the reference
474 assembly using TBLASTN (E-value <= 1E-5)[60]. Then the candidate gene regions were
475 refined by GeneWise[61] for more accurate splicing sites and gene models. We randomly
476 selected 1000 homology-based genes to train Augustus[62] for *de novo* prediction on the
477 pre-masked genome sequences. We mapped RNA-seq reads of 13 samples to the genome
478 using TopHat (v1.3.1)[63] and then assembled the transcripts by Cufflinks (v1.3.0)
479 (http://cufflinks.cbcb.umd.edu/). Transcripts from different samples were merged by
480 Cuffmerge. Finally, gene models from these three methods were combined into a
481 non-redundant gene set.
482 We finally obtained 21,194 protein-coding genes with intact open reading frames
483 (ORFs) **(Supplementary Table 14)**. The gene models (measured by gene length, mRNA
484 length, exon number and exon length) are comparable to those of other vertebrates and
485 are well supported by the RNA-Seq data **(Supplementary Figure 18 and**
486 **Supplementary Table 5).** To annotate the gene names for each predicted protein-coding
487 locus, we first mapped all the 21,194 genes to a manually collected Ensembl gene library,
488 which consists of all proteins from *Anolis carolinensis, Gallus gallus, Homo sapiens,*
489 *Xenopus tropicalis and Danio rerio.* Then the best hit of each snake gene was retained
490 based on its BLAST alignment score, and the gene name of this best hit gene was
491 assigned to the query snake gene. Most of the predicted genes can be found for their
492 orthologous genes in the library at a threshold of 80% alignment rate (the aligned length
493 divided by the original protein length), suggesting our annotation has a high quality
494 **(Supplementary Table 15)**.
495

496 **RNA-seq and gene expression analyses**

497 Total RNAs were isolated from four types of tissues collected from both sexes, including
498 brain, liver, venom gland and gonad **(Supplementary Table 16).** RNA sequencing

499 libraries were constructed using the Illumina mRNA-Seq Prep Kit. Briefly, oligo(dT)
500 magnetic beads were used to purify poly-A containing mRNA molecules. The mRNAs
501 were further fragmented and randomly primed during the first strand synthesis by reverse
502 transcription. This procedure was followed by a second-strand synthesis with DNA
503 polymerase I to create double-stranded cDNA fragments. The cDNAs were subjected to
504 end-repairing by Klenow and T4 DNA polymerases and A-tailed by Klenow lacking
505 exonuclease activity. The fragments were ligated to Illumina Paired-End Sequencing
506 adapters, size selected by gel electrophoresis and then PCR amplified to complete the
507 library preparation. The paired-end libraries were sequenced using Illumina HiSeq 2000
508 (90/100 bp at each end).
509 We used TopHat (v1.3.1) for aligning the RNA-seq reads and predicting the splicing
510 junctions with the following parameters: -I/--max-intron-length: 10000, --segment-length:
511 25, --library-type: fr-firststrand, --mate-std-dev 10, -r/--mate-inner-dist: 20. Gene
512 expression was measured by reads per kilobase of gene per million mapped reads
513 (RPKM). To minimize the influence of different samples, RPKMs were adjusted by a
514 scaling method based on TMM (trimmed mean of M values; M values mean the log
515 expression ratios)[64] which assumes that the majority of genes are common to all samples
516 and should not be differentially expressed.
517

518 **Evolution analyses**

519 A phylogenetic tree of the five-pacer viper and the other sequenced genomes (*Xenopus*
520 *tropicalis, Homo sapiens, Mus musculus, Gallus gallus, Chelonia mydas, Alligator*
521 *mississippiensis, Anolis carolinensis, Boa constrictor, Python bivittatus* and *Ophiophagus*
522 *hannah*) was constructed using the 5,353 orthologous single-copy genes. Treebest
523 (http://treesoft.sourceforge.net/treebest.shtml) was used to construct the phylogenetic tree.
524 To estimate the divergence times between species, for each species, 4-fold degenerate
525 sites were extracted from each orthologous family and concatenated to one sequence for
526 each species. The MCMCtree program implemented in the Phylogenetic Analysis by
527 Maximum Likelihood (PAML)[65] package was used to estimate the species divergence
528 time. Calibration time was obtained from the TimeTree database

529 (http://www.timetree.org/). Three calibration points were applied in this study as normal
530 priors to constrain the age of the nodes described below. 61.5-100.5 MA for the most
531 recent common ancestor (TMRCA) of human-mouse; 259.7-299.8 MA for TMRCA of
532 Crocodylidae and Lepidosauria; 235- 250.4 MA for TMRCA of Aves and Crocodylidae[66].
533 To examine the evolution of gene families in Squamate reptiles, genes from four
534 snakes (*Boa constrictor, Python bivittatus, Deinagkistrodon acutus, Ophiophagus*
535 *hannah*) and green anole lizard were clusterred into gene families by Treefam
536 (min_weight=10, min_density=0.34, and max_size=500) [67]. The family expansion or
537 contraction analysis was performed by CAFE[68]. In CAFE, a random birth-and-death
538 model was proposed to study gene gain and loss in gene families across a user-specified
539 phylogenetic tree. A global parameter λ (lambda), which described both gene birth (λ)
540 and death ($\mu = -\lambda$) rate across all branches in the tree for all gene families was estimated
541 using maximum likelihood method. A conditional p-value was calculated for each gene
542 family, and the families with conditional p-values lower than 0.05 were considered to
543 have a significantly accelerated rate of expansion and contraction.
544 For the PAML analyses, we first assigned orthologous relationships for 12,657 gene
545 groups among all Squamata and outgroup (turtle) using the reciprocal best blast hit
546 algorithm and syntenic information. We used PRANK[69] to align the orthologous gene
547 sequences, which takes phylogenetic information into account when placing a gap into
548 the alignment. We filtered the PRANK alignments by gblocks[70] and excluded genes with
549 high proportion of low complexity or repetitive sequences to avoid alignment errors. To
550 identify the genes that evolve under positive selection (PSGs), we performed likelihood
551 ratio test (LRT) using the branch model by PAML[65]. We first performed a LRT of the
552 two-ratio model, which calculates the dN/dS ratio for the lineage of interest and the
553 background lineage, against the one-ratio model assuming a uniform dN/dS ratio across all
554 branches, so that to determine whether the focal lineage is evolving significantly faster
555 (p-value < 0.05). In order to differentiate between episodes of positive selection and
556 relaxation of purifying selection (RSGs), we performed a LRT of two-ratios model
557 against the model that fixed the focal lineage's dN/dS ratio to be 1 (p-value < 0.05) and
558 also required PSGs with the free-ratio model dN/dS > 1 at the focal lineage. For the

559 identified RSGs and PSGs, we used their mouse orthologs' mutant phenotype
560 information[71] and performed enrichment analyses using MamPhEA[72]. Then we grouped
561 the enriched MP terms by different tissue types.
562
563 **Olfactory receptor (OR), *Hox* and venom gene annotation**
564 To identify the nearly complete functional gene repertoire of OR, *Hox* and venom toxin
565 genes in the investigated species, we first collected known amino acid sequences of 458
566 intact OR genes from three species (green anole lizard, chicken and zebra finch)[73], all
567 annotated *Hox* genes from *Mus musculus* and *HoxC3* from *Xenopus tropicalis*, and
568 obtained the query sequences of a total of 35 venom gene families[74] from UniProt
569 (http://www.uniprot.org/) and NCBI (http://www.ncbi.nlm.nih.gov/). These 35 venom
570 gene families represent the vast majority of known snake venoms. Then we performed a
571 TBlastN[60] search with the cutoff E-value of 1E-5 against the genomic data using these
572 query sequences. Aligned sequence fragments were combined into one predicted gene
573 using perl scripts if they belonged to the same query protein. Then each candidate gene
574 region was extended for 2kb from both ends to predict its open reading frame by
575 GeneWise[61]. Obtained sequences were verified as corresponding genes by BlastP
576 searches against NCBI nonredundant (nr) database. Redundant annotations within
577 overlapped genomic regions were removed.
578 For the OR gene prediction, these candidates were classified into functional genes
579 and nonfunctional pseudogenes. If a sequence contained any disruptive frame-shift
580 mutations and/or premature stop codons, it was annotated as a pseudogene. The
581 remaining genes were examined using TMHMM2.0[75]. Those OR genes containing more
582 at least 6 transmembrane (TM) structures were considered as intact candidates and the
583 rest were also considered as pseudogenes. Finally, each OR sequence identified was
584 searched against the HORDE (the Human Olfactory Data Explorer) database
585 (http://genome.weizmann.ac.il/horde/) using the FASTA (ftp://ftp.virginia.edu/pub/fasta)
586 and classified into the different families according to their best-aligned human OR
587 sequence. For the venom toxin genes, we only kept these genes with RPKM higher than 1
588 in the five-pacer viper and king cobra venom gland tissue as final toxin gene set.

589

590 **Identification and analyses of sex-linked genes**

591 To identify the Z-linked scaffolds in the male assembly, we aligned the female and male
592 reads to the male genome separately with BWA[58] allowing 2 mismatches and 1 indel.
593 Scaffolds with less than 80% alignment coverage (excluding gaps) or shorter than 500 bp
594 in length were excluded. Then single-base depths were calculated using SAMtools[76], with
595 which we calculated the coverage and mean depth for each scaffold. The expected male
596 vs. female (M:F) scaled ratio of a Z-linked scaffold is equal to 2, and we defined a
597 Z-linked scaffold with the variation of an observed scaled ratio to be less than 20% (i.e.
598 1.6 to 2.4). With this criteria, we identified 139 Z-lined scaffolds, representing 76.93Mb
599 with a scaffold N50 of 962 kb (**Supplementary Table 17**). These Z-linked scaffolds were
600 organized into pseudo-chromosome sequence based on their homology with green anole
601 lizard. Another characteristic pattern of the Z-linked scaffolds is that there should be
602 more heterozygous SNPs in the male individual than in the female individual resulted
603 from their hemizygous state in female. We used SAMtools[76] for SNP/indel calling. SNPs
604 and indels whose read depths were too low (<10) or too high (>120), or qualities lower
605 than 100 were excluded. As expected, the frequency of heterozygous sites of Z
606 chromosome of the female individual is much lower than that of the male individual
607 (0.005% vs 0.08%), while the heterozygous rate of autosomes are similar in both sex
608 (~0.1%) (**Supplementary Table 18**). To identify the W-linked scaffolds, we used the
609 similar strategy as the Z-linked scaffold detection to obtain the coverage and mean depth
610 of each scaffold. Then we identified those scaffolds covered by female reads over 80% of
611 the length, and by male reads with less than 20% of the length. With this method, we
612 identified 33 Mb W-linked scaffolds with a scaffold N50 of 48 kb (**Supplementary Table**
613 **19**).

614 We used the protein sequences of Z/W gametologs from garter snake and pygmy
615 rattle snake[12] as queries and aligned them to the genomes of boa (the SGA assembly,
616 http://gigadb.org/dataset/100060), five-pacer viper and king cobra with BLAST[60]. The
617 best aligned (cutoff: identity>=70%, coverage>=50%) region with extended flanking
618 sequences of 5kb at both ends was then used to determine whether it contains an intact

open reading frame (ORF) by GeneWise[61] (-tfor -genesf -gff -sum). We annotated the ORF as disrupted when GeneWise reported at least one premature stop codon or frame-shift mutation. CDS sequences of single-copy genes' Z/W gametologs were aligned by MUSCLE[77] and the resulting alignments were cleaned by gblocks[70] (-b4=5, -t=c, -e=-gb). Only alignments longer than 300bp were used for constructing maximum likelihood trees by RAxML[78] to infer whether their residing evolutionary stratum is shared among species or specific to lineages.

References

1 Greene, H. W. *Snakes: the evolution of mystery in nature*. (Univ of California Press, 1997).

2 Tchernov, E., Rieppel, O., Zaher, H., Polcyn, M. J. & Jacobs, L. L. A fossil snake with limbs. *Science* **287**, 2010-2012 (2000).

3 Cohn, M. J. & Tickle, C. Developmental basis of limblessness and axial patterning in snakes. *Nature* **399**, 474-479, doi:10.1038/20944 (1999).

4 Apesteguia, S. & Zaher, H. A Cretaceous terrestrial snake with robust hindlimbs and a sacrum. *Nature* **440**, 1037-1040, doi:10.1038/nature04413 (2006).

5 Gracheva, E. O. *et al.* Molecular basis of infrared detection by snakes. *Nature* **464**, 1006-1011, doi:10.1038/nature08943 (2010).

6 Vonk, F. J. *et al.* Evolutionary origin and development of snake fangs. *Nature* **454**, 630-633, doi:10.1038/nature07178 (2008).

7 Di-Poi, N. *et al.* Changes in Hox genes' structure and function during the evolution of the squamate body plan. *Nature* **464**, 99-103, doi:10.1038/nature08789 (2010).

8 Guerreiro, I. *et al.* Role of a polymorphism in a Hox/Pax-responsive enhancer in the evolution of the vertebrate spine. *Proc Natl Acad Sci U S A* **110**, 10682-10686, doi:10.1073/pnas.1300592110 (2013).

9 Fry, B. G. From genome to "venome": molecular origin and evolution of the snake venom proteome inferred from phylogenetic analysis of toxin sequences and related body proteins. *Genome Res* **15**, 403-420, doi:10.1101/gr.3228405

649 (2005).
650 10 Vonk, F. J. *et al.* The king cobra genome reveals dynamic gene evolution and
651 adaptation in the snake venom system. *Proc Natl Acad Sci U S A* **110**,
652 20651-20656, doi:10.1073/pnas.1314702110 (2013).
653 11 Fry, B. G., Vidal, N., van der Weerd, L., Kochva, E. & Renjifo, C. Evolution and
654 diversification of the Toxicofera reptile venom system. *J Proteomics* **72**, 127-136,
655 doi:10.1016/j.jprot.2009.01.009 (2009).
656 12 Vicoso, B., Emerson, J. J., Zektser, Y., Mahajan, S. & Bachtrog, D. Comparative
657 sex chromosome genomics in snakes: differentiation, evolutionary strata, and lack
658 of global dosage compensation. *PLoS Biol* **11**, e1001643,
659 doi:10.1371/journal.pbio.1001643 (2013).
660 13 Ohno, S. *Sex Chromosomes and Sex-linked Genes*. Vol. 1967 (Springer Berlin
661 Heidelberg, 1967).
662 14 Kaiser, V. B. & Bachtrog, D. Evolution of sex chromosomes in insects. *Annu Rev*
663 *Genet* **44**, 91-112, doi:10.1146/annurev-genet-102209-163600 (2010).
664 15 Westergaard, M. The mechanism of sex determination in dioecious flowering
665 plants. *Adv Genet* **9**, 217-281 (1958).
666 16 Castoe, T. A. *et al.* The Burmese python genome reveals the molecular basis for
667 extreme adaptation in snakes. *Proc Natl Acad Sci U S A* **110**, 20645-20650,
668 doi:10.1073/pnas.1314475110 (2013).
669 17 Woltering, J. M. *et al.* Axial patterning in snakes and caecilians: evidence for an
670 alternative interpretation of the Hox code. *Dev Biol* **332**, 82-89,
671 doi:10.1016/j.ydbio.2009.04.031 (2009).
672 18 Head, J. J. & Polly, P. D. Evolution of the snake body form reveals homoplasy in
673 amniote Hox gene function. *Nature* **520**, 86-89, doi:10.1038/nature14042 (2015).
674 19 Gomez, C. *et al.* Control of segment number in vertebrate embryos. *Nature* **454**,
675 335-339, doi:10.1038/nature07020 (2008).
676 20 Zhang, B. *et al.* Transcriptome analysis of Deinagkistrodon acutus venomous
677 gland focusing on cellular structure and functional aspects using expressed
678 sequence tags. *BMC Genomics* **7** (2006).

679 21 Bradnam, K. R. *et al.* Assemblathon 2: evaluating de novo methods of genome
680 assembly in three vertebrate species. *Gigascience* **2**, 10,
681 doi:10.1186/2047-217X-2-10 (2013).
682 22 Lin, X. *et al.* The effect of the fibrinolytic enzyme FIIa from Agkistrodon acutus
683 venom on acute pulmonary thromboembolism. *Acta Pharmacologica Sinica* **32**,
684 239-244 (2011).
685 23 Li, Z. *et al.* Comparison of the two major classes of assembly algorithms:
686 overlap-layout-consensus and de-bruijn-graph. *Brief Funct Genomics* **11**, 25-37,
687 doi:10.1093/bfgp/elr035 (2012).
688 24 Alfoldi, J. *et al.* The genome of the green anole lizard and a comparative analysis
689 with birds and mammals. *Nature* **477**, 587-591, doi:10.1038/nature10390 (2011).
690 25 Pyron, R. A. & Burbrink, F. T. Extinction, ecological opportunity, and the origins
691 of global snake diversity. *Evolution* **66**, 163-178,
692 doi:10.1111/j.1558-5646.2011.01437.x (2012).
693 26 Yunfang, Q., Xingfu, X., Youjin, Y., Fuming, D. & Meihua., H. Chromosomal
694 studies on six species of venomous snakes in Zhejiang. *Acta Zoologica Sinica* **273**,
695 218-227 (1981).
696 27 Srikulnath, K. *et al.* Karyotypic evolution in squamate reptiles: comparative gene
697 mapping revealed highly conserved linkage homology between the butterfly
698 lizard (Leiolepis reevesii rubritaeniata, Agamidae, Lacertilia) and the Japanese
699 four-striped rat snake (Elaphe quadrivirgata, Colubridae, Serpentes). *Chromosome*
700 *Res* **17**, 975-986, doi:10.1007/s10577-009-9101-7 (2009).
701 28 Yang, Z. Likelihood ratio tests for detecting positive selection and application to
702 primate lysozyme evolution. *Mol Biol Evol* **15**, 568-573 (1998).
703 29 Martill, D. M., Tischlinger, H. & Longrich, N. R. EVOLUTION. A four-legged
704 snake from the Early Cretaceous of Gondwana. *Science* **349**, 416-419,
705 doi:10.1126/science.aaa9208 (2015).
706 30 Held, J. *How the Snake Lost Its Legs: Curious Tales from the Frontier of*
707 *Evo-Devo*. (Cambridge University Press, 2014).
708 31 Xu, B. *et al.* Hox5 interacts with Plzf to restrict Shh expression in the developing

709 forelimb. *Proc Natl Acad Sci U S A* **110**, 19438-19443,
710 doi:10.1073/pnas.1315075110 (2013).
711 32 Boulet, A. M. & Capecchi, M. R. Multiple roles of Hoxa11 and Hoxd11 in the
712 formation of the mammalian forelimb zeugopod. *Development* **131**, 299-309,
713 doi:10.1242/dev.00936 (2004).
714 33 King, M., Arnold, J. S., Shanske, A. & Morrow, B. E. T-genes and limb bud
715 development. *Am J Med Genet A* **140**, 1407-1413, doi:10.1002/ajmg.a.31250
716 (2006).
717 34 Logan, M. & Tabin, C. J. Role of Pitx1 upstream of Tbx4 in specification of
718 hindlimb identity. *Science* **283**, 1736-1739 (1999).
719 35 Wellik, D. M. & Capecchi, M. R. Hox10 and Hox11 genes are required to
720 globally pattern the mammalian skeleton. *Science* **301**, 363-367,
721 doi:10.1126/science.1085672 (2003).
722 36 McGrew, M. J., Dale, J. K., Fraboulet, S. & Pourquie, O. The lunatic fringe gene
723 is a target of the molecular clock linked to somite segmentation in avian embryos.
724 *Curr Biol* **8**, 979-982 (1998).
725 37 Muragaki, Y., Mundlos, S., Upton, J. & Olsen, B. R. Altered growth and
726 branching patterns in synpolydactyly caused by mutations in HOXD13. *Science*
727 **272**, 548-551 (1996).
728 38 Kaske, S. *et al.* TRPM5, a taste-signaling transient receptor potential ion-channel,
729 is a ubiquitous signaling component in chemosensory cells. *BMC Neuroscience* **8**,
730 49 (2007).
731 39 Dehara, Y. *et al.* Characterization of squamate olfactory receptor genes and their
732 transcripts by the high-throughput sequencing approach. *Genome Biol Evol* **4**,
733 602-616, doi:10.1093/gbe/evs041 (2012).
734 40 Khan, I. *et al.* Olfactory receptor subgenomes linked with broad ecological
735 adaptations in Sauropsida. *Mol Biol Evol* **32**, 2832-2843,
736 doi:10.1093/molbev/msv155 (2015).
737 41 Hayden, S. *et al.* A cluster of olfactory receptor genes linked to frugivory in bats.
738 *Mol Biol Evol* **31**, 917-927, doi:10.1093/molbev/msu043 (2014).

739 42 Daltry, J. C., Wuster, W. & Thorpe, R. S. Diet and snake venom evolution. *Nature*
740 **379**, 537-540, doi:10.1038/379537a0 (1996).
741 43 Hargreaves, A. D., Swain, M. T., Hegarty, M. J., Logan, D. W. & Mulley, J. F.
742 Restriction and recruitment-gene duplication and the origin and evolution of
743 snake venom toxins. *Genome Biol Evol* **6**, 2088-2095, doi:10.1093/gbe/evu166
744 (2014).
745 44 Casewell, N. R., Harrison, R. A., Wuster, W. & Wagstaff, S. C. Comparative
746 venom gland transcriptome surveys of the saw-scaled vipers (Viperidae: Echis)
747 reveal substantial intra-family gene diversity and novel venom transcripts. *BMC*
748 *Genomics* **10**, 564, doi:10.1186/1471-2164-10-564 (2009).
749 45 Matsubara, K. *et al.* Evidence for different origin of sex chromosomes in snakes,
750 birds, and mammals and step-wise differentiation of snake sex chromosomes.
751 *Proc Natl Acad Sci U S A* **103**, 18190-18195, doi:10.1073/pnas.0605274103
752 (2006).
753 46 Ohno, S. *Sex chromosomes and sex-linked genes*. Vol. 1 (Springer, 1967).
754 47 Zhou, Q. *et al.* Complex evolutionary trajectories of sex chromosomes across bird
755 taxa. *Science* **346**, 1246338, doi:10.1126/science.1246338 (2014).
756 48 Cortez, D. *et al.* Origins and functional evolution of Y chromosomes across
757 mammals. *Nature* **508**, 488-493, doi:10.1038/nature13151 (2014).
758 49 Nicolas, M. *et al.* A gradual process of recombination restriction in the
759 evolutionary history of the sex chromosomes in dioecious plants. *PLoS Biol* **3**, e4,
760 doi:10.1371/journal.pbio.0030004 (2005).
761 50 Li, W. H., Yi, S. & Makova, K. Male-driven evolution. *Curr Opin Genet Dev* **12**,
762 650-656 (2002).
763 51 Vicoso, B. & Charlesworth, B. Evolution on the X chromosome: unusual patterns
764 and processes. *Nat Rev Genet* **7**, 645-653, doi:10.1038/nrg1914 (2006).
765 52 Mank, J. E. The W, X, Y and Z of sex-chromosome dosage compensation. *Trends*
766 *Genet* **25**, 226-233, doi:10.1016/j.tig.2009.03.005 (2009).
767 53 Boucherat, O. *et al.* Partial functional redundancy between Hoxa5 and Hoxb5
768 paralog genes during lung morphogenesis. *Am J Physiol Lung Cell Mol Physiol*

769 **304**, L817-L830 (2013).
770 54 Guerreiro, I. & Duboule, D. Snakes: hatching of a model system for Evo-Devo?
771 *Int J Dev Biol* **58**, 727-732, doi:10.1387/ijdb.150026dd (2014).
772 55 Booth, W., Johnson, D. H., Moore, S., Schal, C. & Vargo, E. L. Evidence for
773 viable, non-clonal but fatherless Boa constrictors. *Biol Lett* **7**, 253-256,
774 doi:10.1098/rsbl.2010.0793 (2011).
775 56 Li, R. *et al.* The sequence and de novo assembly of the giant panda genome.
776 *Nature* **463**, 311-317, doi:10.1038/nature08696 (2010).
777 57 Luo, R. *et al.* SOAPdenovo2: an empirically improved memory-efficient
778 short-read de novo assembler. *Gigascience* **1**, 18, doi:10.1186/2047-217X-1-18
779 (2012).
780 58 Li, H. & Durbin, R. Fast and accurate short read alignment with Burrows-Wheeler
781 transform. *Bioinformatics* **25**, 1754-1760, doi:10.1093/bioinformatics/btp324
782 (2009).
783 59 Jurka, J. Repbase update: a database and an electronic journal of repetitive
784 elements. *Trends Genet* **16**, 418-420 (2000).
785 60 Altschul, S. F., Gish, W., Miller, W., Myers, E. W. & Lipman, D. J. Basic local
786 alignment search tool. *J Mol Biol* **215**, 403-410,
787 doi:10.1016/S0022-2836(05)80360-2 (1990).
788 61 Birney, E., Clamp, M. & Durbin, R. GeneWise and Genomewise. *Genome Res* **14**,
789 988-995, doi:10.1101/gr.1865504 (2004).
790 62 Stanke, M., Steinkamp, R., Waack, S. & Morgenstern, B. AUGUSTUS: a web
791 server for gene finding in eukaryotes. *Nucleic Acids Res* **32**, W309-312,
792 doi:10.1093/nar/gkh379 (2004).
793 63 Trapnell, C., Pachter, L. & Salzberg, S. L. TopHat: discovering splice junctions
794 with RNA-Seq. *Bioinformatics* **25**, 1105-1111, doi:10.1093/bioinformatics/btp120
795 (2009).
796 64 Robinson, M. D. & Oshlack, A. A scaling normalization method for differential
797 expression analysis of RNA-seq data. *Genome Biol* **11**, R25,
798 doi:10.1186/gb-2010-11-3-r25 (2010).

799 65 Yang, Z. PAML 4: phylogenetic analysis by maximum likelihood. *Mol Biol Evol*
800 **24**, 1586-1591, doi:10.1093/molbev/msm088 (2007).
801 66 Benton, M. J. & Donoghue, P. C. Paleontological evidence to date the tree of life.
802 *Mol Biol Evol* **24**, 26-53, doi:10.1093/molbev/msl150 (2007).
803 67 Li, H. *et al.* TreeFam: a curated database of phylogenetic trees of animal gene
804 families. *Nucleic Acids Res* **34**, D572-580, doi:10.1093/nar/gkj118 (2006).
805 68 De Bie, T., Cristianini, N., Demuth, J. P. & Hahn, M. W. CAFE: a computational
806 tool for the study of gene family evolution. *Bioinformatics* **22**, 1269-1271,
807 doi:10.1093/bioinformatics/btl097 (2006).
808 69 Loytynoja, A. & Goldman, N. An algorithm for progressive multiple alignment of
809 sequences with insertions. *Proc Natl Acad Sci U S A* **102**, 10557-10562,
810 doi:10.1073/pnas.0409137102 (2005).
811 70 Talavera, G. & Castresana, J. Improvement of phylogenies after removing
812 divergent and ambiguously aligned blocks from protein sequence alignments. *Syst*
813 *Biol* **56**, 564-577, doi:10.1080/10635150701472164 (2007).
814 71 Bult, C. J. *et al.* Mouse genome database 2016. *Nucleic Acids Res* **44**, D840-847,
815 doi:10.1093/nar/gkv1211 (2016).
816 72 Weng, M. P. & Liao, B. Y. MamPhEA: a web tool for mammalian phenotype
817 enrichment analysis. *Bioinformatics* **26**, 2212-2213,
818 doi:10.1093/bioinformatics/btq359 (2010).
819 73 Steiger, S. S., Kuryshev, V. Y., Stensmyr, M. C., Kempenaers, B. & Mueller, J. C.
820 A comparison of reptilian and avian olfactory receptor gene repertoires:
821 species-specific expansion of group gamma genes in birds. *BMC Genomics* **10**,
822 446, doi:10.1186/1471-2164-10-446 (2009).
823 74 Mackessy, S. P. *Handbook of venoms and toxins of reptiles*. (CRC Press, 2016).
824 75 Krogh, A., Larsson, B., von Heijne, G. & Sonnhammer, E. L. Predicting
825 transmembrane protein topology with a hidden Markov model: application to
826 complete genomes. *J Mol Biol* **305**, 567-580, doi:10.1006/jmbi.2000.4315 (2001).
827 76 Li, H. *et al.* The Sequence Alignment/Map format and SAMtools. *Bioinformatics*
828 **25**, 2078-2079, doi:10.1093/bioinformatics/btp352 (2009).

829 77 Edgar, R. C. MUSCLE: multiple sequence alignment with high accuracy and high
830 throughput. *Nucleic Acids Res* **32**, 1792-1797, doi:10.1093/nar/gkh340 (2004).
831 78 Stamatakis, A. RAxML version 8: a tool for phylogenetic analysis and
832 post-analysis of large phylogenies. *Bioinformatics* **30**, 1312-1313,
833 doi:10.1093/bioinformatics/btu033 (2014).
834

835 **Figure Legend**

836 **Figure 1.** The comparative genomic landscape of five-pacer viper

837 (**A**) *Deinagkistrodon acutus* (five-pacer viper) and eight adult tissues used in this study.

838 (**B**) Circos plot showing the linkage group assignment using lizard chromosomes as

839 reference (outmost circle), normalized female vs. male mapped read coverage ratio (blue

840 line) and GC-isochore structures of five-pacer viper (red), boa (yellow) and green anole

841 lizard (green). Both snake genomes have a much higher variation of local GC content

842 than that of green anole lizard. (**C**) Phylogenomic tree constructed using fourfold

843 degenerate sites from 8006 single-copy orthologous genes. We also showed bootstrapping

844 percentages, the numbers of inferred gene family expansion (in green) and contraction

845 (red), and corresponding phylogenetic terms at each node. MRCA: most recent common

846 ancestor.

847

848 **Figure 2.** Genomic and transcriptomic variation of snake transposable elements

849 **(A)** Violin plots showing each type of TE's frequency distribution of sequence divergence

850 level from the inferred ancestral consensus sequences. Clustering of TEs with similar

851 divergence levels, manifested as the 'bout' of the violin, corresponds to the burst of TE

852 amplification. **(B)** Bar plots comparing the genome-wide TE content between four snake

853 species. TE families were annotated combining information of sequence homology and

854 *de novo* prediction. **(C)** TE's average normalized expression level (measured by RPKM)

855 across different tissues in five-pace viper.

856

857 **Figure 3.** Evolution of snake genes and gene families

858 (**A**) Phylogenetic distribution of mutant phenotypes (MP) of mouse orthologs of snakes.

859 Each MP term is shown by an organ icon, and significantly enriched for snake genes

860 undergoing positive selection (red) or relaxed selective constraints (gray) inferred by

861 lineage-specific PAML analyses. (**B**) We show the four *Hox* gene clusters of snakes,

862 with each box showing the ratio of nonsynonymous (dN) over synonymous substitution

863 (dS) rate at the snake ancestor lineage. White boxes represent genes that haven't been

864 calculated for their ratios due to the genome assembly issue in species other than

865 five-pacer viper. Boxes with dotted line refer to genes with dS approaching 0, therefore
866 the dN/dS ratio cannot be directly shown. Each cluster contains up to 13 *Hox* genes with
867 some of them lost during evolution. We also marked certain *Hox* genes undergoing
868 positive selection (in red) or relaxed selective constraints (in green) at a specific lineage
869 above the box. Each lineage was denoted as: S: *Serpentes* (ancestor of all snakes), H:
870 *Henophidia* (ancestor of boa and python), B: *Boa constrictor*, P: *Python bivittatus*, C:
871 *Colubroidea*, D: *Deinagkistrodon acutus*, O: *Ophiophagus hannah*. (**C**) Comparing
872 olfactory receptor (OR) gene repertoire between boa, viper and lizard. Each cell
873 corresponds to a certain OR family (shown at y-axis) gene number on a certain
874 chromosome (x-axis). (**D**) Pie chart shows the composition of normalized venom gland
875 transcripts of male five-pacer viper. The heatmap shows the normalized expression level
876 (in RPKM) across different tissues of viper and king cobra. We grouped the venom genes
877 by their time of origination, shown at the bottom x-axis.
878
879 **Figure 4.** Snake sex chromosomes have at least three evolution strata
880 The three tracks in the top panel shows female read depths along the Z chromosome
881 relative to the median depth value of autosomes, Z/W pairwise sequence divergence
882 within intergenic regions, and female read depths of W-linked sequence fragments
883 relative to the median depth value of autosomes. Depths close to 1 suggest that the region
884 is a recombining pseudoautosomal region (PAR), whereas depths of 0.5 are expected in a
885 highly differentiated fully sex-linked region where females are hemizygous. The
886 identifiable W-linked fragments are much denser at the region 56Mb~70Mb, probably
887 because this region (denoted as stratum 3, S3) has suppressed recombination most
888 recently. S2 and S1 were identified and demarcated by characterizing the sequence
889 conservation level (measured by LASTZ alignment score, blue line) between the chrZs of
890 boa and viper. At the oldest stratum S1 where recombination has been suppressed for the
891 longest time, there is an enrichment of repetitive elements on the affected Z-linked region
892 (Gypsy track in red, 100kb non-overlapping sliding window). And these Z-linked TEs A
893 similar pattern was found in homologous recombining region of boa, but not in lizard.
894

895 **Supplementary Figure Legend**

896 **Supplementary Figure 1.** K-mer estimation of the genome size of five-pacer viper.
897 Distribution of 17-mer frequency in the used sequencing reads from female (left) and
898 male (right) samples. The x-axis represents the sequencing depth. The Y-axis represents
899 the proportion of a *K*-mer counts in total *K*-mer counts at a given sequencing depth. The
900 estimated genome size is about 1.43 Gb.

901

902 **Supplementary Figure 2.** GC isochore structure of different tetrapod genomes.
903 We show the standard deviation (SD) of GC content calculated with different window
904 size (3 kb to 320 kb) for different vertebrate genomes.

905

906 **Supplementary Figure 3.** Comparing expression levels of genes nearby expressed TEs
907 in each tissue.
908 We show expression patterns of genes around highly expressed TE (RPKM > 5) in
909 different tissues from both sexes, including brain, liver, venom gland and gonad. We also
910 performed comparison between the focal tissue vs. the other tissues. We show levels of
911 significance with asterisks. *: 0.001=< *P*-value <0.01; **: 0.0001 =< *P*<0.001; ***:
912 *P*<0.0001.

913

914 **Supplementary Figure 4.** Comparison of *Hox* gene structure between snakes and lizard.
915 Schematic representation of four *Hox* clusters in anole lizard, boa, Burmese python,
916 five-pacer viper and king cobra. Each number from 1 to 13 denotes the specific *Hox* gene
917 belonging to one cluster. We showed the length difference between each species vs.
918 mouse by the colored lines (for intergenic regions) or boxes (for intronic regions): a
919 1.5~3 fold increase of length was shown by blue, a more than 3-fold increase was shown
920 in red. Exons were shown by vertical lines, and dotted lines refer to exons with unknown
921 boundaries, either due to assembly issues. Double-slashes refer to the gap between two
922 different scaffolds.

923

924 **Supplementary Figure 5.** Repeat accumulation at *Hox* gene clusters.

925 Comparison of the TE and simple repeat content of *Hox* cluster genes with 5kb flanking
926 regions between snakes and lizard. We calculated the repeat density by dividing the total
927 length of specific repeat sequence vs. the length of corresponding region. This density was
928 normalized over the genome-wide repeat density and then shown by heatmap.
929
930 **Supplementary Figure 6.** Phylogenetic distribution of enriched MP terms.
931 We identified enriched mutant phenotypes (MP) of mouse orthologs of snake genes that
932 are undergoing lineage-specific positive selection (red) and relaxed selective constraints
933 (gray). And then we mapped these MP terms onto the snake phylogeny.
934
935 **Supplementary Figure 7.** Read coverage density plot of different linkage groups.
936 For each linkage group (from left to right, chrW, chrZ, chr1), male reads were plotted in
937 blue, and female reads in red. The identified chrW scaffolds in this work all show a
938 female-specific read depth pattern.
939
940 **Supplementary Figure 8.** Male-driven evolution effect in snakes.
941 For each gene, we calculated the substitution rates between anole lizard and each of boa,
942 Burmese python, five-pacer viper and king cobra at synonymous sites (dS) and
943 non-synonymous sites (dN) divided into different chromosome sets. To detect
944 branch-specific differences, we obtained for each gene the ratios of these evolutionary
945 rates between the different snake species vs. boa. Since boa's homologous chromosomal
946 region to the Z chromosomes of other advanced snakes represent the ancestral status of
947 snake sex chromosomes, a higher relative ratios of Z-linked dS of advanced snakes vs.
948 boa than those of autosomes indicate the male-driven evolution effect. We shown the
949 Wilcoxon test significant differences between the Z chromosome and the autosomes
950 (chr1-5) are marked with asterisks (***, P-value < 0.001).
951
952 **Supplementary Figure 9.** Repeat accumulation along the snake sex chromosomes.
953 Shown are comparisons of the distribution of Gypsy, CR1 and L1 content along the
954 chromosome in anole lizard, Boa and five-pacer viper. The TE content was calculated by

955 averaging the TE density of each sliding window of 100kb as well as the flanking 10
956 windows.
957
958 **Supplementary Figure 10.** Gene trees for Z and W linked gametologs in S1 region.
959 Shown are maximum likelihood (ML) trees using coding regions of Z and W allelic
960 sequences from multiple snake species, with the gene name under each tree and
961 bootstrapping values at each node. Trees that show separate clustering of Z- or W- linked
962 gametologs provide strong evidence that these genes suppressed recombination before the
963 speciation.
964
965 **Supplementary Figure 11.** Gene trees for Z and W linked gametologs in S2 region.
966
967 **Supplementary Figure 12.** Gene trees for Z and W linked gametologs in S3 region.
968
969 **Supplementary Figure 13.** Comparison of repeat content between viper chrZ and chrW.
970 TE families were determined based on the combined annotations of Repbase,
971 RepeatModeler, and coverage in the genome was annotated using in-house scripts.
972
973 **Supplementary Figure 14.** Comparison of gene expression across different
974 chromosomes.
975 We show gene expression patterns between different chromosome sets across tissues.
976 'pseudo-W' refers to W-linked genes that have premature stop codons or frameshift
977 mutations
978
979 **Supplementary Figure 15.** Pairwise comparison of gene expression levels between
980 homologous Z and W alleles.
981
982 **Supplementary Figure 16.** Gene expression along the Z chromosome and autosome
983 chr5 in different tissues of five-pacer viper.
984 We show log-based male-to-female gene expression ratio along the Z chromosomes and

985 autosome chr5. Only genes with RPKM >= 1 in both the male and female were
986 considered. If genes are mostly non-biased, the line is expected to centered at 0. The
987 pattern indicates five-pacer viper lacks chromosome-wide dosage compensation.
988
989 **Supplementary Figure 17.** Frequency distribution of sequencing depth.
990 Distribution of sequencing depth of the assembled female (left) and male (right) genomes
991 by reads from the female and male samples. The peak depth is 76X and 77X for the
992 female and male reads aligned to corresponding assembly, respectively.
993
994 **Supplementary Figure 18.** Comparisons of gene parameters among the sequenced
995 representative species.
996 We used the published genomes of *Gallus gallus, Homo sapiens, Anolis carolinensis,*
997 *Boa constrictor* to compare with *Deinagkistrodon acutus*, without finding any obvious
998 differences between them and five-pacer viper in the annotated genes' length and number.
999 This indicates the high quality of gene annotation.
1000
1001 **Supplementary Table Legend**
1002 **Supplementary Table 1.** Statistics of five-pacer viper genome sequencing.
1003
1004 **Supplementary Table 2.** Statistics of 17-mer analysis.
1005
1006 **Supplementary Table 3.** Statistics of reads of small-insert and large-insert libraries
1007 aligned to the male assembly.
1008 *PE mapped* refer to reads being mapped to the genome as read pairs, and *SE mapped*
1009 represent reads being mapped to the genome as single reads.
1010
1011 **Supplementary Table 4.** Summary of the five-pacer viper genome assemblies.
1012
1013 **Supplementary Table 5.** Number of expressed genes of five-pacer viper.
1014
1015 **Supplementary Table 6.** Number of genes and scaffold size organized into
1016 chromosomes.
1017

1018 **Supplementary Table 7.** Comparison of repeat content between snakes and lizard.

1019

1020 **Supplementary Table 8.** Comparison of genome assembly quality between snakes and

1021 lizard.

1022

1023 **Supplementary Table 9.** Evolution of candidate limb-patterning genes in snakes.

1024 Candidate limb-patterning genes were collected from MGI database and published paper.

1025 Genes undergoing positive selection (P) or relaxed selective constraints (R), were

1026 identified by PAML analyses. N: there is no significant selection signal. '-' refers to

1027 genes that cannot be completely assembled for their coding sequences due to genome

1028 assembly gaps.

1029

1030 **Supplementary Table 10. Comparison of venom genes between snakes.**

1031 Statistics of venom gene families in the four snakes and anole lizard genomes based on

1032 homology-based prediction. AVIT: Prokineticin; C3: complement C3; CVF: Cobra

1033 Venom Factor; CRISPs: Cysteine-Rich Secretory Proteins; Hy: Hyaluronidases;

1034 Natriuretic: Natriuretic peptide; NGF: Snake Venom Nerve Growth Factors; PLA2-2A:

1035 Snake Venom Phospholipase A2 (type IIA); SVMP: Snake Venom Metalloproteinases;

1036 TL: thrombin-like snake venom serine proteinases; LAAO: Snake Venom L-Amino Acid

1037 Oxidases; PDE: phosphodiesterases; CLPs: snake C-type lectin-like proteins; VEGF:

1038 vascular endothelin growth factor; PLA2-1B: Snake Venom Phospholipase A2 (type IB);

1039 3FTX: The three-finger toxins; ACeH: Acetylcholinesterase;

1040

1041 **Supplementary Table 11.** Comparison of repeat content between snake sex

1042 chromosomes and their lizard homolog.

1043

1044 **Supplementary Table 12.** Location of W-linked putative pseudogenes.

1045

1046 **Supplementary Table 13.** Fractions of bases covered by reads in the male assembly.

1047

1048 **Supplementary Table 14.** Characteristics of predicted protein-coding genes in the male

assembly.

Supplementary Table 15. Number of predicted genes that can find homologs in the Ensembl library with different aligning rate cutoff.
Alignment rate was calculated by dividing the aligned length vs. the original protein length. And we required both the query and subject to satisfy our alignment cutoff. The Ensembl library consists of all proteins from Anolis carolinensis, Gallus gallus, Homo sapiens, Xenopus tropicalis and Danio rerio.

Supplementary Table 16. Data production and alignment statistic of RNA-Seq aligned to male genome assembly.

Supplementary Table 17. Statistics of the identified Z-linked scaffolds.

Supplementary Table 18. Statistics of SNPs identified in the female and male individual.

Supplementary Table 19. Statistics of identified W-linked scaffolds**.**

Supplementary Data Legend

Supplementary Data 1

Comparing five-pacer viper's chromosomal assignment vs. reported fluorescence in situ hybridization results.

Supplementary Data 2

GO enrichment of nearby genes of TE highly expressed in brain.

Supplementary Data 3

Positively selected genes (PSGs) and genes with relaxed selective constraints (RSGs) and their affected lineage.

Supplementary Data 4

Mouse mutant terms' enrichment analyses of PSGs and RSGs across different snake branches.

Supplementary Data 5

GO enrichment of expanded and contracted gene families across different snake lineages.

Supplementary Data 6

Plots of GO enrichment of expanded and contracted gene families using Ontologizer.

Acknowledgement

We would like to thank Ren-jie Wang for sharing the snake photo, and three anonymous reviewers for their valuable comments. This project was supported by the Thousand Young Talents Program funding, and a startup funding of Life Science Institute of Zhejiang University to Q. Z., and National Major Scientific and Technological Special Project for 'Significant New Drugs Development' during the Twelfth Five-year Plan Period (No. 2009ZX09102-217, 2009-2010) to W. Y. All the raw reads, genome assembly and annotation generated in this study are deposited under the BioProject # PRJNA314370 on NCBI.

Author Contribution

Q.Z., W.Y., G.Y. conceived and supervised the project. B.L., P.Q., W.Z., Y.H. and X.S. provided and extracted the samples. Z.L. and B.W. performed the proteomic mass spectrometry-based experiment and data analysis. J.L., Z.W. and Y.Z. performed the genome assembly and annotation. J.L. and Q.L. designed and performed the identification of sex-linked scaffolds. P.Z. performed RNA-seq data analysis. Z.W., L.J. and Y.Z. performed the genome evolution analyses. Z.W., Y.Z., L.J. and B.Q. performed genes and gene family evolution analyses. Z.W. and L.J. performed the sex chromosome evolution analyses. Q.Z., Z.W., G.Z., G.Y. interpreted the results and wrote the manuscript. All of the authors read and approved the final manuscript.

1111 **Figure 1.** The comparative genomic landscape of five-pace viper

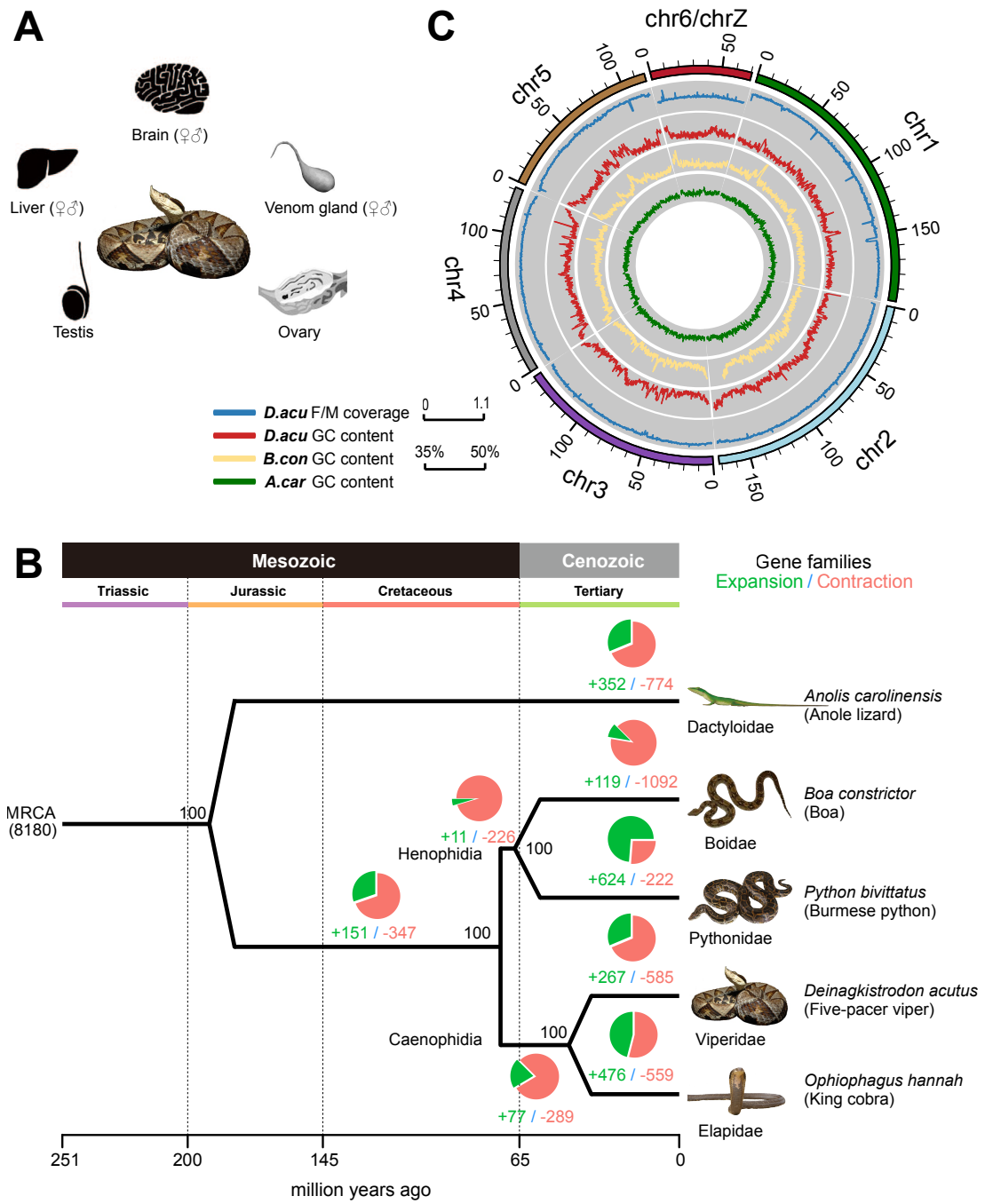

1112

1113

1114 **Figure 2.** Genomic and transcriptomic variation of snake transposable elements

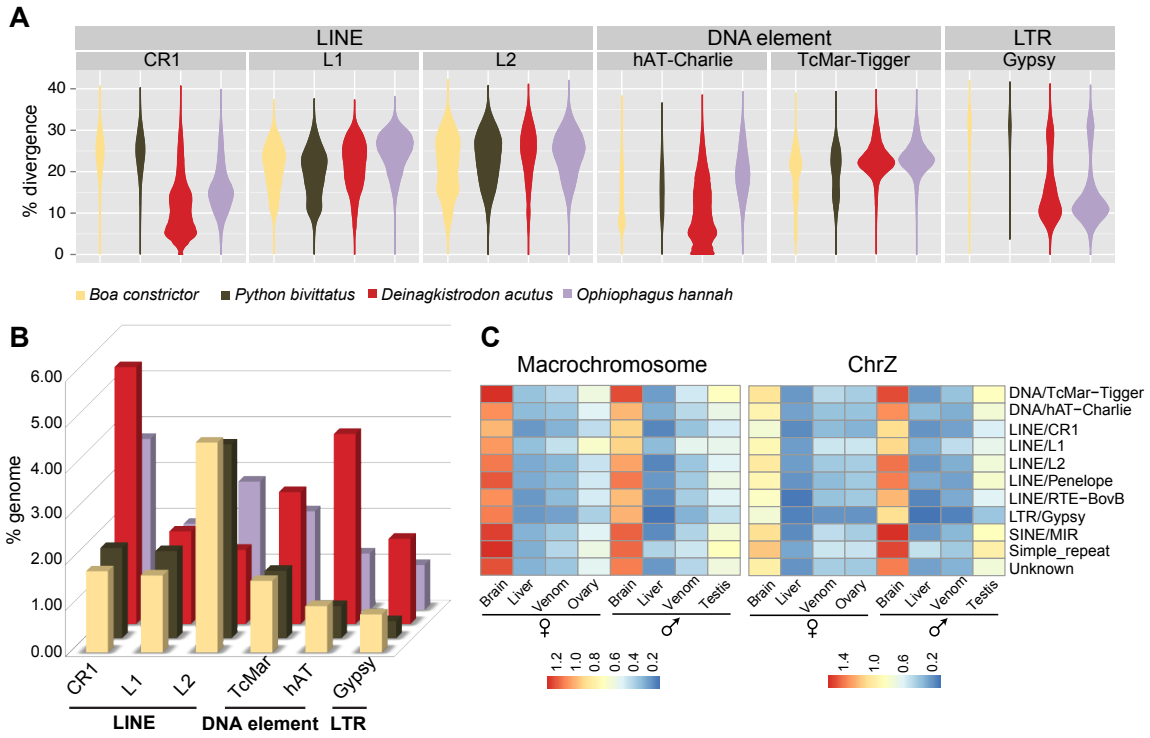

1115

1116

Figure 3. Evolution of snake genes and gene families

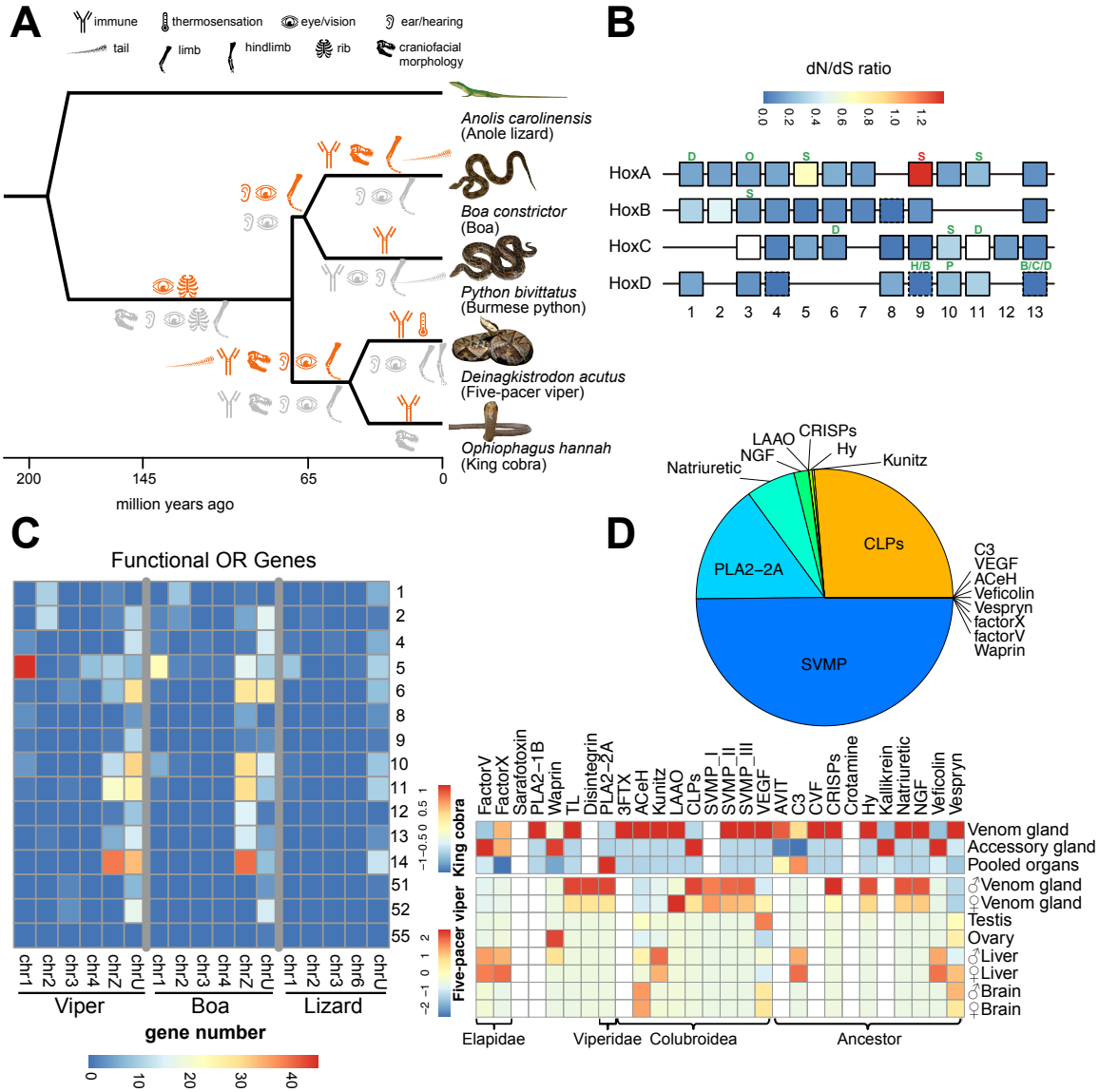

1119 **Figure 4.** Snake sex chromosomes have at least three evolution strata

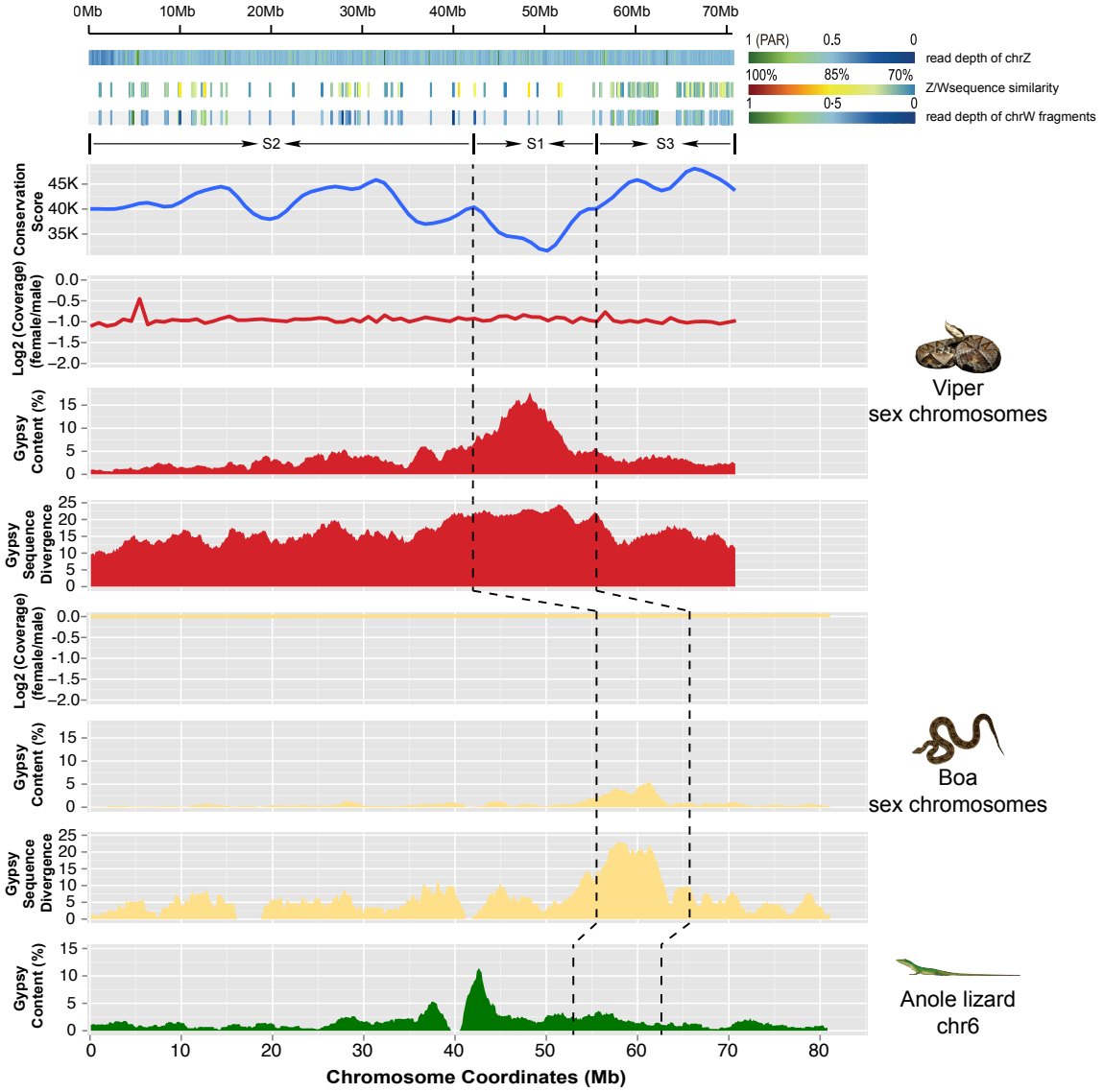

1120